Scale-up of Pneumatic Conveying Systems in Existing Plants

Peter Hilgraf[1], Jan Paepcke[2], Marieke Moka[3] and Arne Hilck[3]
1. Senior Process Technology Manager
2. Head of Territory Sales Management
3. Process Technology Manager
Claudius Peters Projects, Buxtehude, Germany
Corresponding author: arne.hilck@claudiuspeters.com
https://doi.org/10.71659/icsoba2024-al014

Abstract

Due to their versatility, pneumatic conveying systems are in use in several bulk handling plants worldwide. With small mechanical changes existing plants can be upgraded or extended. The efficiency of the new version is then not in any case optimized. A simple model to scale up pneumatic conveying systems is described to verify the efficiency of newly modified conveying systems.

Based on given dimension and existing field data the energy consumption of a conveying plant is calculated first. Then the ideal version for the task is calculated and the two version are compared. The engineering model allows for an easy monitoring of existing and new systems.

Keywords: Pneumatic conveying, Energy efficiency.

1. Summary

A method for transferring the conveying pressure losses determined on a pneumatic test system to an operating system that differs in geometry and routing is presented. For this purpose, the $\overline{Fr}_R = \bar{v}_F^2/(g \cdot D_R)$ variation of the total test resistance coefficient, which is related to an average Froude number and depends on the pipe routing, is converted into a resistance coefficient of the solid that is (as far as possible) independent of the pipeline route $\bar{\lambda}_{S,h,V}(\overline{Fr}_R) = \bar{\lambda}_{S,h,B}(\overline{Fr}_R)$ and thus can be used for scale-up. From this, in turn, the respective total drag coefficient of the current plant $\lambda_{tot,B}$ can be determined, taking into account the course/characteristics of the operating system.

The procedure described is comprehensively illustrated on the basis of the measurement results of two bulk materials that are very different in their conveying behavior - wood powder and limestone powder. At the end a scale-up is done for an example with alumina.

2. Introduction

In the case of orientating conveying tests in a test plant (L_R, D_R), which are intended to assess the fundamental suitability of a new/not yet pneumatically conveyed bulk material, usually only the mass flows of solids $\dot{M}_S$ and conveyed gas $\dot{M}_F$ as well as the total pressure loss $|\Delta p_R|$ given back pressure p_{out} are usually measured as a function of the respective operating conditions at the beginning and end of the pipeline, i.e. the pressures (p_{in}, p_{out}), the gas velocities $(v_{F,in}, v_{F,out})$ and the loading $\mu = \dot{M}_S/\dot{M}_F$, with: $\dot{M}_S, \dot{M}_F =$ solids, gas mass flow, detected by measurement. The same conditions usually also apply to operating facilities in which the operator realizes different load cases, e.g., by varying the parameters mentioned. From the measured variables determined in this way, the adjusted pressure loss equation can be used to:

$$|\Delta p_R| = \lambda_{tot} \cdot \mu \cdot \frac{L_R}{D_R} \cdot \frac{\bar{\varrho}_F}{2} \cdot \bar{v}_F^2 \quad (1)$$

where:

Δp_R	Total pressure drop of conveying line, *bar*
λ_{tot}	Total resistance coefficient
μ	Specific load, kg_S/kg_F
L_R	Length of piping, *m*
D_R	Diameter of piping, *mm*
$\bar{\varrho}_F$	Mean conveying gas density, kg/m^3
$\bar{v}_F$	Mean "empty pipe velocity" of gas, *m/s*

An overall resistance coefficient λ_{tot} of the current production can be calculated. $\bar{v}_F$ is a suitably defined mean gas velocity, $\bar{\varrho}_F$ the corresponding mean conveying gas density. Both will be discussed in more detail. The λ_{tot}-values of the operating conditions examined at the test line describe their respective average pressure loss resistance and contain the individual resistances of the present conveyor line, i.e., they are pipeline-specific and cannot be used directly for the design of deviating conveying lines.

In the following, a method for transferring these "summarized" test results to operating systems is presented, which differ geometrically from the test routing, e.g., regarding pipe length L_R, pipe inner diameter D_R and/or route. The quality of the transfer is checked with the help of measurement results of the bulk materials wood flour and limestone powder.

The following stipulation applies:

- u_X refers to true velocities, "v_X" to so-called "empty pipe velocities. For the gas phase in pneumatic pipelines, for example $v_F = \varepsilon_F \cdot u_F$ applies, with ε_F relative voidage volume of the gas. Since such systems have values, $\varepsilon_F \gtrsim 0.90$. $u_F = v_F$ can generally be set with reasonable accuracy. In test evaluations in practice, this assumption is usually always used.

3. Pressure Loss Calculation of Pneumatic Conveying Lines

The following section introduces the equations required to calculate the pressure loss of pneumatic conveying lines. This is followed by a description of the usual procedure in practice for determining this total pressure loss.

The total pressure loss of a pipe consisting of horizontal and vertical pipe sections as well as the surrounding conveyor line is additively composed of the proportions of

$$\begin{aligned} \Delta p_R = \textstyle\sum_{i=1}^{n} \Delta p_i = {} & \Delta p_{S,f,h}\ \text{(Solid friction horizontal)} + \\ & \Delta p_{S,f,v}\ \text{(Solid friction vertical)} + \\ & \Delta p_{S,Hub}\ \text{(Solids lifting)} + \\ & \Delta p_{S,acc}\ \text{(Solids Acceleration)} + \\ & \textstyle\sum \Delta p_{S,U}\ \text{(Sum of solid deflections)} + \\ & \Delta p_F\ \text{(Conveying gas)} \end{aligned} \quad (2)$$

together. For the individual terms, cf. e.g., [1]. The terms in Equation (2) are described in the following sections.

3.1 Solid Friction, Horizontal Straight Tube

For an incompressible conveying in the inertia state, the following follows from a balance of forces on the solid in analogy to the single-phase flow:

$$-\Delta p_{S,f,h} = \varepsilon_F \cdot \lambda_{S,h} \cdot \mu \cdot \frac{\Delta L_{R,h}}{D_R} \cdot \frac{\varrho_F}{2} \cdot u_F^2 \cong \lambda_{S,h} \cdot \mu \cdot \frac{\Delta L_{R,h}}{D_R} \cdot \frac{\varrho_F}{2} \cdot v_F^2 \quad (3)$$

where:

$\Delta p_{S,f,h}$	Pressure loss solid friction horizontal, *bar*
ε_F	Relative voidage volume of gas
$\lambda_{S,h}$	Resistance coefficient, horizontal
μ	Specific load, kg_S/kg_F
L_R	Length of piping, *m*
D_R	Diameter of piping, *mm*
$\bar{\varrho}_F$	Mean conveying gas density, *kg/m³*
$\bar{u}_F$	True mean velocity of gas, *m/s*

Theoretically, $\lambda_{S,h}$, the resistance coefficient, can be further resolved into two additive components: a particle/pipe wall impact including particle/particle impact share $\lambda_{Stoß}$ and a wall friction share β_R due to sliding solid strands or plugs supporting themselves on the pipe sheet or pipe walls. In production tests, however, only the total value $\lambda_{S,h}$ can be determined by direct measurement.

The $\lambda_{S,h}$-values are measured by tests on short horizontal pipe sections ΔL_R (→ incompressible flow) with correspondingly long inlet and outlet sections to ensure an undisturbed flow. For the given bulk material, one can represent or correlate $\lambda_{S,h}$ as a function of the local Froude numbers $Fr_R = v_F^2/(g \cdot D_R)$, with: g =gravitational acceleration ($= 9.81\ m/s^2$). Measurements show that $\lambda_{S,h}$ it not only depends on the Fr_R-number, but is also influenced, especially in the case of fine-grained bulk materials, by the load μ and, if necessary, the size of the conveyor pipe diameter D_R. $\lambda_{S,h}$decreases at constant values of (μ, D_R) with increasing Fr_R-number and runs into a limit value at high Fr_R, while at constant Fr_R values it takes on smaller values with increasing load μ and larger pipe diameter D_R.

Horizontal solids friction is usually the dominant proportion of the total pressure loss $|\Delta p_R|$ of a conveyor line.

3.2 Solid Friction, Vertical Straight Tube

The calculation approach for $\Delta p_{S,f,v}$ is identical to that of the Eq. (3):

$$-\Delta p_{S,f,v} = \varepsilon_F \cdot \lambda_{S,v} \cdot \mu \cdot \frac{\Delta L_{R,v}}{D_R} \cdot \frac{\varrho_F}{2} \cdot u_F^2 \cong \lambda_{S,v} \cdot \mu \cdot \frac{\Delta L_{R,v}}{D_R} \cdot \frac{\varrho_F}{2} \cdot v_F^2 \quad (4)$$

where:

$\Delta p_{S,f,v}$	Pressure loss solid friction vertical, *bar*
ε_F	Relative voidage volume of gas
$\lambda_{S,v}$	Resistance coefficient, vertical
μ	Specific load, kg_S/kg_F
$L_{R,v}$	Length of vertical section of piping, *m*
D_R	Diameter of piping, *mm*

$\bar{\varrho}_F$ Mean conveying gas density, *kg/m³*
$\bar{u}_F$ True mean velocity of gas, *m/s*

Since in vertical pipes there are essentially only shock/impact losses and no sliding friction losses, the vertical drag coefficient $\lambda_{S,v}$ is generally smaller than $\lambda_{S,h}$ in horizontal lines. This can be described by

$$\lambda_{S,v} \cong k_v \cdot \lambda_{S,h} \quad \rightarrow \quad with: \ 0.5 \lesssim k_v \leq 1{,}0 \tag{5}$$

where:
$\lambda_{S,v}$ Resistance coefficient, vertical
$\lambda_{S,h}$ Resistance coefficient, horizontal
k_v Factor reflecting the specific load

In the dense phase range, i.e., with higher loads μ, k_v-values of the order of magnitude $k_v \cong 0.5$ are determined. With decreasing μ, i.e., transition to the lean phase conveying area, $k_v \rightarrow 1$ occurs. It follows from this that the frictional pressure loss of a vertical conveyor line can be determined as that of a horizontal pipe of the same length operated under identical boundary conditions. However, with a drag coefficient reduced by a factor k_v. Thus, the following applies:

$$\Delta p_{S,f,v} \cong k_v \cdot \Delta p_{S,f,h} \tag{6}$$

where:
$\Delta p_{S,f,h}$ Pressure loss solid friction horizontal, *bar*
$\Delta p_{S,f,v}$ Pressure loss solid friction vertical, *bar*
k_v Factor reflecting the specific load

$\lambda_{S,v}$ can be determined in the same way as $\lambda_{S,h}$, but the pressure loss measured via the considered pipe element must be reduced by the additional stroke pressure loss (→ see "solids lifting").

3.3 Solids Lifting

The weight $(\Delta M_S \cdot g)$ of the solid mass $\Delta M_S = \dot{M}_S \cdot \overline{\Delta t}_S = \dot{M}_S \cdot \Delta L_{R,v}/\bar{u}_S$ currently in the vertical conveyor pipe (→ the buoyancy is neglected, since $\varrho_F \ll \varrho_S$) must be borne by the pressure differential force$\left(-\Delta p_{S,Hub} \cdot A_R\right)$, A_R = pipe cross-section. $\overline{\Delta t}_S$ is the mean residence time of the solids in the lifting section. From this, after some conversions with $\varepsilon_F = 1$ and $u_F \cong v_F$

$$-\Delta p_{S,Hub} \cong \frac{g}{\bar{C}_v} \cdot \frac{\dot{M}_S \cdot \Delta L_{R,v}}{A_R \cdot \bar{v}_F} = \frac{g}{\bar{C}_v} \cdot \mu \cdot \bar{\varrho}_F \cdot \Delta L_{R,v} \quad \rightarrow$$

$$with: \ \bar{C}_v = \bar{u}_S/\bar{u}_F \cong \bar{u}_S/\bar{v}_F \tag{7}$$

where:
$\Delta p_{S,Hub}$ Pressure loss solids lifting, *bar*
g Gravity acceleration, 9.81 *kg m/s²*
$\bar{C}_v$ Ratio of solid and conveying gas velocities
$\dot{M}_S$ Mass flow solid*, t/h*
μ Specific load, kg_S/kg_F
L_R Length of piping, *m*
D_R Diameter of piping, *mm*
$\bar{\varrho}_F$ Mean conveying gas density, *kg/m³*
$\bar{v}_F$ Mean "empty pipe velocity" of gas, *m/s*

$\bar{u}_s$ True mean velocity of solid, m/s

The swept values are average values over the considered lifting height $\Delta L_{R,v}$. $\bar{C}_v$ describes the average velocity ratio of solids and conveying gas, $\bar{\varrho}_F$ the average gas density.

3.4 Solids Acceleration

The solids entering the conveyor line at the axial speed $u_{s,in} = 0$ must first be accelerated to its stationary inertia velocity at the beginning of the pipeline $u_{S,stat} = C_{in} \cdot u_{F,in}$ and then further along the conveyor line to the respective current differential/slip speed to the expanding conveying gas. The application of the momentum theorem

$$-\Delta p_{S,acc} \cdot A_R = \dot{M}_S \cdot \Delta u_S \tag{8}$$

where:

$\Delta p_{S,acc}$ Pressure loss solids acceleration, *bar*
A_R Area of pipe, *m²*
$\dot{M}_S$ Mass flow solid, *t/h*
Δu_s True velocity of solid, *m/s*

Leads with $u_{S,in} = 0$ and thus $\Delta u_S = u_{S,out} = C_{out} \cdot u_{F,out} \cong C_{out} \cdot v_{F,out}$ to the acceleration pressure loss of the solids along the entire conveyor line.

$$-\Delta p_{S,acc} \cong \dot{M}_S \cdot \frac{(C_{out} \cdot v_{F,out})}{A_R} \tag{9}$$

where:

$\Delta p_{S,acc}$ Pressure loss solids acceleration, *bar*
A_R Area of pipe, *m²*
$\dot{M}_S$ Mass flow solid, *t/h*
$v_{F,out}$ Gas velocity at outlet, *m/s*

C_{out} is the velocity ratio of solids and conveyed gas at the end of the pipeline.

3.5 Solids Deflection

When the flow direction of the gas-solid mixture changes, the inertia of the solid particles and the centrifugal forces acting on them lead to an almost complete separation of gas and solid. The strand of solids pressed against the outside of the deflector (→ coarse-grained hard particles can also cause a rebound) is slowed down by the increased wall friction to $u_{S,U,out}$ and must be accelerated back to its original inertia speed $u_{S,U,in}$ behind the deflection. The application of the impulse theorem, Equation (8), leads with

$$\Delta u_S = \left(u_{S,U,in} - u_{S,U,out}\right) = \left(\frac{\Delta u_{S,U}}{u_{S,U,in}}\right) \cdot u_{S,U,in} = K_U \cdot C_{U,in} \cdot u_{F,U,in} \cong K_U \cdot C_{U,in} \cdot v_{F,U,in}$$

on

$$-\Delta p_{S,U} \cong K_U \cdot C_{U,in} \cdot \frac{\dot{M}_S \cdot v_{F,U,in}}{A_R} = K_U \cdot C_{U,in} \cdot \mu \cdot \varrho_{F,U,in} \cdot v_{F,U,in}^2 \tag{10}$$

where:

$\Delta u_{S,U}$	Solid velocity difference between inlet and outlet, *m/s*
$u_{S,U,out}$	Outlet solid velocity (at deflection), *m/s*
$u_{S,U,in}$	Initial solid velocity (at deflection), *m/s*
$v_{F,in}$	Gas velocity at inlet, *m/s*
$v_{F,out}$	Gas velocity at outlet, *m/s*
ρ_F	Conveying gas density, *kg/m³*
K_U	Relative solid decelaration´
C_U	Ratio of solid and conveying gas velocity
μ	Specific load, kg_S/kg_F
A_R	Area of piping, *m²*
$\bar{v}_F$	Mean "empty pipe velocity" of gas, *m/s*
$\bar{u}_F$	True mean velocity of gas, *m/s*
ε_F	Relative voidage volume of gas

Quantities indicated with " in " refer to the condition at the entrance to the deflector. The magnitude of relative solids deceleration

$$K_U = \frac{\Delta u_{S,U}}{u_{S,U,in}} = \frac{u_{S,U,in} - u_{S,U,out}}{u_{S,U,in}} = 1 - \frac{u_{S,U,out}}{u_{S,U,in}} \tag{11}$$

depends, among other things, on the properties of the bulk material, the design of the deflection (→ tube arches, deflection cup, T-bend, etc.) and its spatial arrangement (→ horizontal, from horizontal to vertical upwards, etc.). The K_U-values of pipe bends arranged horizontally with arbitrary deflection angles α_U and a wall friction angle φ_W between pipe wall and bulk material can be calculated with

$$K_U = 1 - exp\left(-\frac{\alpha_U}{180°} \cdot \pi \cdot \beta_R\right) \quad \rightarrow \quad with: \ \beta_R = \tan \varphi_W \tag{12}$$

where:

K_u	Solids deflection factor
α_U	Angle of the bend, °
β_R	Wall friction coefficient
φ_w	Wall friction angle, °

If conveying is carried through ($\alpha_U = 90°$)-pipe bends arranged in this way, the following values can be used in Equation (10):

- Fine-grained bulk material: $\left(K_U \cdot C_{U,in}\right)_{90°RB} \cong 0.35$
- Coarse-grained bulk material: $\left(K_U \cdot C_{U,in}\right)_{90°RB} \cong 0.25$
- Vortex deflector: fine-grained bulk material.$\left(K_U \cdot C_{U,in}\right)_{Vortex} \cong 0.434$

Further details and related literature can be found in [1].

3.6 Pressure Loss Conveying Gas

Since the conveying gas itself rubs against the pipe wall, may flow through installations (→ resistance coefficient ξ_i), has to be deflected and accelerated and lifted, this results in a loss of inherent pressure. The proportion of gas in the total pressure loss of a pneumatic conveying is negligible in the case of denser conveyances, i.e., loads $\mu \gtrsim 15$, but must be taken into account

in the case of air conveying with lower loads. In general, only the frictional pressure loss $\Delta p_{F,f}$ and the acceleration pressure loss $\Delta p_{F,acc}$ of the gas are essential, i.e., with $u_F \cong v_F$.

$$-\Delta p_F \cong -\left(\Delta p_{F,f} + \Delta p_{F,acc}\right) \cong \bar{\lambda}_F \cdot \frac{L_R}{D_R} \cdot \frac{\bar{\varrho}_F}{2} \cdot \bar{v}_F^2 + \dot{M}_F \cdot \frac{\left(v_{F,out} - v_{F,in}\right)}{A_R} \qquad (13)$$

where:

Δp_F	Pressure loss gas, *bar*
$\Delta p_{F,f}$	Pressure loss, friction, *bar*
$\Delta p_{F,acc}$	Pressure loss, gas acceleration, *bar*
λ_F	Friction coefficient
L_R	Length of piping, *m*
D_R	Diameter of piping, *mm*
$\bar{\varrho}_F$	Mean conveying gas density, *kg/m³*
$\dot{M}_F$	Mass flow conveying gas, *kg/h*
$v_{F,in}$	Gas velocity at inlet, *m/s*
$v_{F,out}$	Gas velocity at outlet, *m/s*
A_R	Free area, *m²*

$\bar{\lambda}_F, \bar{\varrho}_F$ and $\bar{v}_F$ are suitably averaged characteristic values for the pipe friction resistance, the density and the velocity of the conveying gas. The Eq. (13) presupposes that the conveying gas behaves as if the solids were not present. Of course, this is not the case: the presence of the bulk particles changes the flow profile and thus the frictional pressure loss. However, this cannot be measured directly in funding trials. Usually, therefore, an undisturbed gas flow is expected approximately.

In order to determine the pressure curve and thus the gas and solids velocity profile along the conveyor line L_R using the Δp_R-model described above, L_R is divided into correspondingly short ΔL_R-sections and pipe elements, e.g., deflections. These are generally calculated element-by-element incompressible using the equations given above, since the back pressure p_{out} is specified there and the corresponding gas velocity $v_{F,out}$ is relatively freely selectable. The continuous courses of (p, v_F, u_S) are thus approximated by staircases. The smaller their jumps, i.e., the ΔL_R-length sections, are chosen, the more accurate the calculation, but the greater the calculation effort. Depending on the accuracy requirements, this calculation, which is incompressible in sections, also requires iterative calculation steps, e.g., to determine the local acceleration pressure losses of gas and solid.

4. Scale up-Model

4.1 Modelling

The use of the standard model described in section 2 requires knowledge of the curves of the local drag coefficients of the two-phase flow along the conveyor line. These are not given in the measurements described in Section 1, which look at the entire line. Here, only "global" characteristic values λ_{tot} of the respective line are determined. In order to be able to use these results anyway, the following procedure is followed:

From the measured and dependent λ_{tot} on the specific route of the pipeline, an average solid-specific resistance coefficient $\bar{\lambda}_{S,h}$ can be calculated, which is independent of the route and thus transferable to other conveying routes, cf. Eq. (3). The equally scale-up-capable conveying gas-specific wall friction coefficient $\bar{\lambda}_F$, Eq. (13), is determined by well-known clean gas approaches, e.g., the Blasius equation. To determine the characteristic values $\left(\bar{\lambda}_{S,h}, \bar{\lambda}_F\right)$, Eq. (1) and (2) are

equated with Eq. (3 - 13). Since there are always conveyor lines with vertical sections and deflections distributed along the line, the following is specified to simplify the calculations:

- The deflections along the conveyor line are converted into 90° pipe bends. Their number N_U results from the equation

$$N_U = \frac{\sum \alpha_U}{90°} \quad \rightarrow \quad with: \sum \alpha_U = Sum\ of\ all\ deflection\ angles \tag{14}$$

- All lifting sections and 90° pipe bends are flowed through at the average gas velocity $\bar{v}_F$, i.e., moved to the line position of this average velocity, $\bar{v}_F$.
- A uniform average velocity ratio of solids and conveyed gas C, independent of the position along the conveying line, is expected,
- The relative solids deceleration in the 90° pipe bends is calculated with Eq. (12) and $\alpha_U = 90°$ regardless of their spatial arrangement. Thus, the following applies:

$$K_U = K_{U,90°} = 1 - exp\left(-\frac{\pi \cdot \beta_R}{2}\right) \tag{15}$$

where:

N_u	Number of deflections of 90°
K_u	Solids deflection factor
$K_{U,90°}$	Solids deflection factor based on 90°
α_U	Angle of the bend, °
β_R	Wall friction coefficient

With the above assumptions and considering that for $(\bar{\varrho}_F \cdot \bar{v}_F) = \dot{M}_F/A_R$, the following correlation arises for an arbitrarily running conveyor line:

$$\lambda_{tot} = \bar{\lambda}_{S,h} \cdot \left(\frac{L_{R,h}}{L_R} + k_v \cdot \frac{L_{R,v}}{L_R}\right) + \frac{\bar{\lambda}_F}{\mu} + 2 \cdot \frac{D_R}{L_R} \cdot \left(C \cdot \frac{v_{F,out}}{\bar{v}_F} + \frac{1}{\mu} \cdot \frac{v_{F,out} - v_{F,in}}{\bar{v}_F} + N_U \cdot K_U \cdot C\right) + \frac{2}{C} \cdot \frac{L_{R,v}}{L_R} \cdot \frac{g \cdot D_R}{\bar{v}_F^2} \tag{16}$$

where:

λ_{tot}	Total resistance coefficient
$\lambda_{S,h}$	Resistance coefficient, horizontal
L_R	Length of piping, *m*
D_R	Diameter of piping, *mm*
k_v	Factor reflecting the specific load
μ	Specific load, kg_S/kg_F
λ_F	Total friction coefficient
$v_{F,in}$	Gas velocity at inlet, *m/s*
$v_{F,out}$	Gas velocity at outlet, *m/s*
N_u	Number of deflections of 90°
K_u	Solids deflection factor
g	gravity acceleration, 9.81 $kg\ m/s^2$

The individual terms in Eq. (16) are dimensionless expressions/identifiers, as is required for a serious scale-up. Reference values for $C, (K_U \cdot C), k_v$ etc. are given in section 3. $\bar{\lambda}_F$-Values are estimated using Blasius' equation, which is valid for hydraulically smooth pipes in the Reynolds range Re_R relevant here:

$$\bar{\lambda}_F = \frac{0.3164}{Re_R^{1/4}} = 0.3164 \cdot \left(\frac{D_R \cdot \bar{v}_F \cdot \bar{\varrho}_F}{\eta_F}\right)^{-1/4} = 0.3164 \cdot \left(\frac{4}{\pi} \cdot \frac{\dot{M}_F}{D_R \cdot \eta_F}\right)^{-1/4} \quad (17)$$

where:

λ_F	Friction coefficient gas
Re_R	Reynolds Number
v_F	Gas velocity, *m/s*
ρ_F	Gas density, *kg/m³*
η_F	Dynamic viscosity of gas, *Pa*s*
$\dot{M}_F$	Mass flow conveying gas, *kg/h*
D_R	Diameter of piping, *mm*

η_F is the dynamic viscosity of the conveying gas at operating temperature. It is pressure-independent up to approximately 1 MPa (10 bar). Eq. (16) illustrates that the influence of gas friction $\bar{\lambda}_F$ on the overall resistance λ_{tot} decreases rapidly with increasing loading $\left(\rightarrow \bar{\lambda}_F/\mu\right)$.

If systematic tests with different operating settings are carried out on the same conveyor line with the same bulk material, $\bar{\lambda}_{S,h}$ as a function of a Froude number $\overline{Fr}_R = \bar{v}_F^2/(g \cdot D_R)$ formed at the average conveying gas velocity $\bar{v}_F$ can be calculated from Eq. (16) and, if necessary, represented as a parameter with (μ, D_R). These measurement curves form the basis for a scale-up of the pressure loss $|\Delta p_R|$ to other conveyor lines.

4.2 Definition of the Average Conveying Gas Velocity $\bar{v}_F$

To determine a characteristic gas velocity $\bar{v}_F$, under the assumption of ideal gas behavior and a linear decrease in the conveying pressure in the direction of transport (in practice only approximate), the integral mean velocity value $\bar{v}_F = \int_0^{L_R} v_F(L_X) \cdot dL_X/L_R$ is calculated to

$$\bar{v}_F = \frac{v_{F,out} \cdot p_{out}}{|\Delta p_R|} \cdot ln\left(\frac{v_{F,out}}{v_{F,in}}\right) \quad (18)$$

where:

v_F	Gas velocity, *m/s*
p_{out}	Total pressure at outlet, *bar*
$v_{F,in}$	Gas velocity at inlet, *m/s*
$v_{F,out}$	Gas velocity at outlet, *m/s*
Δp_R	Total pressure drop of conveying line, *bar*

Comparisons with the geometric mean value of gas inlet and gas outlet velocities

$$v_{F,geo} = \sqrt{v_{F,in} \cdot v_{F,out}} \quad (19)$$

where:

$v_{F,in}$	Gas velocity at inlet, *m/s*
$v_{F,out}$	Gas velocity at outlet, *m/s*
$v_{F,geo}$	Geometric mean velocity, *m/s*

This differs only slightly from $\bar{v}_F$, cf. Table 1.

Table 1. Comparison of $\bar{v}_F$ and $v_{F,geo}$ at $p_{out} = 1.0\ bar$.

$\lvert\Delta p_R\rvert$ $[bar]$	$v_{F,in}$ $[m/s]$	$v_{F,out}$ $[m/s]$	$\bar{v}_F$ $[m/s]$	$v_{F,geo}$ $[m/s]$
1.00	10.0	20.0	13.86	14.14
1.50	10.0	25.0	15.27	15.81
2.00	5.0	15.0	8.24	8.66
2.00	10.0	30.0	16.48	17.32

In consideration of the real pressure curves and the simpler manageability, the geometrically averaged gas velocity is therefore used as a reference velocity in the following considerations, i.e. $\bar{v}_F = v_{F,geo}$ is set.

4.3 Measurement Results

To illustrate the procedure described, the measurement results for λ_{tot} determined with two very different types of bulk materials and the $\bar{\lambda}_{S,h}$-values calculated backwards from them are presented below. The bulk materials are on the one hand a relatively fine-grained wood powder [2] and on the other hand a very finely ground limestone powder [3]. Both were conveyed under systematically varied operating conditions by pipes with different courses, diameters D_R and lengths L_R.

Table 2 summarizes some of the characteristics of the two bulk materials. The wood powder was transported through the three conveying lines shown in Table 3, while the limestone powder was measured during conveying through the pipes described in Table 4. With the Eq. (16) converted to $\bar{\lambda}_{S,h}$

$$\bar{\lambda}_{S,h} = \frac{\lambda_{tot} - \frac{\bar{\lambda}_F}{\mu} - 2 \cdot \frac{D_R}{L_R} \cdot \left(C \cdot \frac{v_{F,out}}{\bar{v}_F} + \frac{1}{\mu} \cdot \frac{v_{F,out} - v_{F,in}}{\bar{v}_F} + N_U \cdot K_U \cdot C \right) - \frac{2}{C} \cdot \frac{L_{R,v}}{L_R} \cdot \frac{1}{\overline{Fr}_R}}{\left(\frac{L_{R,h}}{L_R} + k_v \cdot \frac{L_{R,v}}{L_R} \right)} \qquad (16a)$$

where:

$\lambda_{S,h}$	Resistance coefficient, horizontal
λ_{tot}	Total resistance coefficient
λ_F	Friction coefficient gas
μ	Specific load, kg_S/kg_F
L_R	Length of piping, m
D_R	Diameter of piping, mm
$\bar{\varrho}_F$	Mean conveying gas density, kg/m^3
$\bar{v}_F$	Mean "empty pipe velocity" of gas, *m/s*
$v_{F,in}$	Gas velocity at inlet, *m/s*
$v_{F,out}$	Gas velocity at outlet, *m/s*
k_v	Factor reflecting the specific load
$\overline{Fr}_R$	Froude number
N_u	Number of deflections of 90°
K_u	Solids deflection factor
$\bar{C}_v$	Ratio of solid and conveying gas velocities

The corresponding solid-specific values $\bar{\lambda}_{S,h}$ can be calculated from the measured data λ_{tot}. In accordance with the present test conditions, the following operating variables were used for the evaluation of the Eq. (16a): Conveying gas = nitrogen (→ wood powder) or ambient air (→ limestone powder), $T_S = 20°C, p_{out} = 1.0\ bar, C = 0.70,\ k_v = 1.00,\ \ (K_U \cdot C) = 0.35,\ \eta_F$, corresponding to the type of gas and temperature.

Table 2. Parameters of the two bulk materials examined.

Parameter	Unit	Wood powder	Limestone powder
Mean particle diameter $d_{S,50}$	$[\mu m]$	291	15
Slope of RRSB Lines α_{RRSB}	[°]	56.2	34.2
Loose bulk density ϱ_{SS}	$[kg/m^3]$	320	1 100
Vibrated Density ϱ_{SR}	$[kg/m^3]$	440	1 680
Solids density ϱ_S	$[kg/m^3]$	1 450	2 720
Deaeration time $\Delta t(2\ kg)$	$[s]$	ca. 6	ca. 50
Geldart Class	[-]	–	C
Particle shape	[-]	flaky, fibrous	rounded, spherical
Notes	[-]	Extreme channel and rat hole formation during fluidization	briquetted, agglomerated

Figure 1 shows the dependencies $\lambda_{tot}(\overline{Fr}_R = \bar{v}_F^2/(g \cdot D_R))$ measured with wood powder on the three pipes examined. The pressure differences on the conveyor lines were varied in the range $\Delta p_R \cong (0.12 \cdots 1.35)\ bar$ and the loads of $\mu \cong (1.0 \cdots 9.0)\ kg_S/kg_F$. only lean phase conveyances with gas velocities of $v_{F,in} \gtrsim\ 17\ m/s$ at the beginning of the pipeline.

Table 3. Conveyor lines examined with wood powder.

Line data		Line 1	Line 2	Line 3
Feeding device		Pressure vessel	Pressure vessel	Screw lock
D_R	mm	54.5	24.0	82.5
L_R	m	63.4	46.6	140.0
$L_{R.v}$	m	7.8	7.9	7.8
$N_{U,90°}$	Eq. (14)	8.0	10.0	11.2

Table 4. Conveyor lines studied with limestone powder.

Line data		Line 1	Line 2	Line 3
Feeding device		Pressure vessel	Pressure vessel	Pressure vessel
D_R	mm	54.5	82.5	82.5
L_R	m	159.0	159.0	62.2
$L_{R.v}$	m	5.8	5.6	6.2
$N_{U.90°}$	Eq. (14)	10.0	10.0	7.0

can be implemented in an operationally reliable manner [3]. The widely differing pipe routings of the three conveying lines results in three different and separate groups of measured values. Based on the explanations in section 2, this was also to be expected.

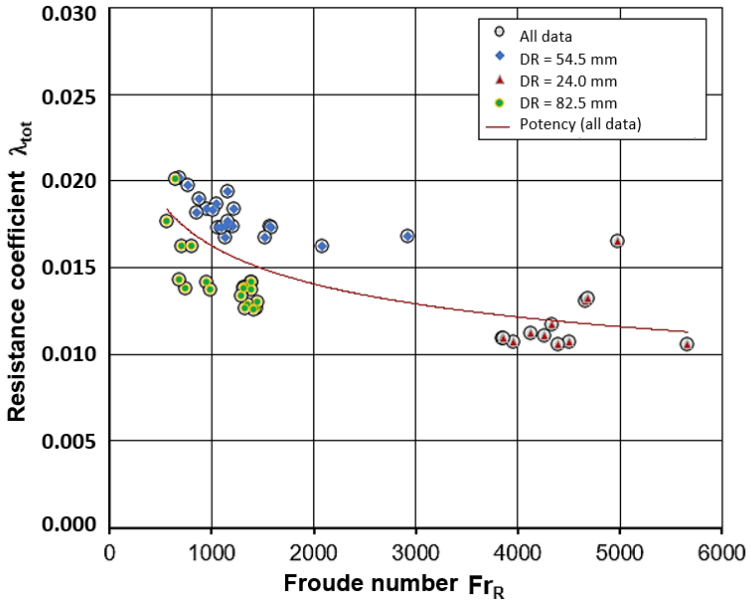

Figure 1. Influence of the special pipe routing on $\lambda_{tot}(\overline{Fr}_R)$ wood powder tests. The curve is for all measured values.

In Figure 2, the scale-up capable horizontal resistance coefficients $\bar{\lambda}_{S,h}$ calculated with Eq. (16a) from the measured λ_{tot}-values are plotted as a function of the geometrically averaged Froude number $\overline{Fr}_R$. In order to be able to clarify details, only the area $\overline{Fr}_R \leq 3000$ is shown. It can be seen that the line diameter D_R exerts an influence on the magnitude of the drag coefficient $\bar{\lambda}_{S,h}$ at a given $\overline{Fr}_R$: With lager D_R, $\bar{\lambda}_{S,h}$ decreases. It should be taken into account that in Figure 2 the ordinate is shown by a factor of 10 smaller than in Figure 1, i.e., the absolute deviations of $\bar{\lambda}_{S,h}$ for variable D_R are relatively small compared to Figure 1. However, as extensive control calculations show, they are real.

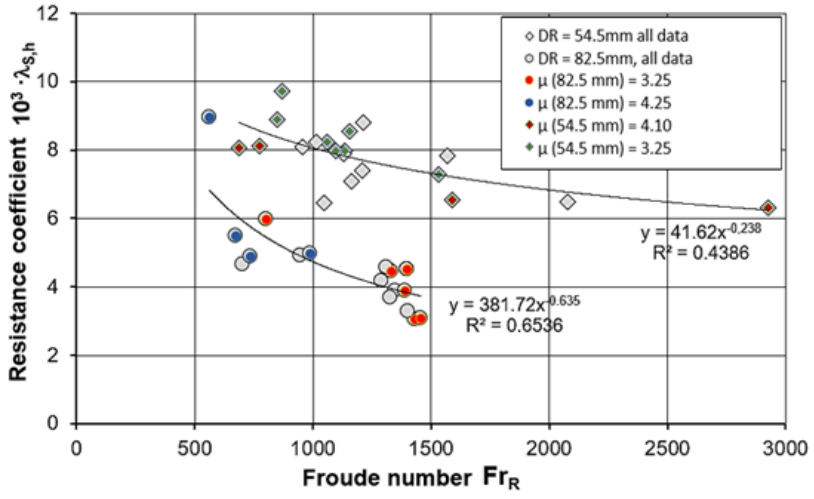

Figure 2. Dependence $\bar{\lambda}_{S,h}(\overline{Fr}_R)$ of wood powder tests $D_R = 54.5\ mm$ and $D_R = 82.5\ mm$. The curves are for all measured values.

This effect can be explained by the fact that the ratio of pipes circumference U_R to the cross-sectional area A_R of the pipe becomes larger with decreasing pipe diameter D_R, i.e. a smaller D_R leads to more frequent particle/pipe wall contacts under comparable operating conditions (→

$e.g.\ \overline{Fr}_R,\ \mu = const.$) and thus cause a greater pressure loss than in a pipe with a larger diameter D_R. The reduction in the $\bar{\lambda}_{S,h}(82.5\,mm)/\bar{\lambda}_{S,h}(54.5\,mm)$-ratio of measured values with increasing pipe diameter D_R depends on the current $\overline{Fr}_R$-number.

A systematic influence of the load μ on $\bar{\lambda}_{S,h}$ is not evident from Figure 2. However, it can be seen that both diameter curves rise very steeply in the area $\overline{Fr}_R \rightarrow 500$ with the higher realized loads μ ($\rightarrow$ is not shown by the compensation curves). This indicates an approximation of the physical production limit, i.e. $\overline{Fr}_R - numbers \lesssim 500$, should not be implemented in operating facilities.

In Figure 3, the limestone powder described in Table 2 is shown at the points described in Table 3 dependencies $\lambda_{tot}(\overline{Fr}_R)$ determined by the lines. The pressure differences on the conveyor lines were varied in the range $\Delta p_R \cong (1.04 \cdots 2.06)\,bar$ and the corresponding loads of $\mu \cong (13.4 \cdots 125.5)\ kg_S/kg_F$. Initial speeds of the conveyor gas down to $v_{F,in} \cong 4.5\ m/s$ were operationally reliable. Thus, transports were realized in both the lean phase and dense phase sectors [3]. A classification into different μ -areas has not been made in Figure 3. The three relatively high measured λ_{tot}-values in the range $\overline{Fr}_R \cong 490$ were determined for conveying with the smallest loads μ.

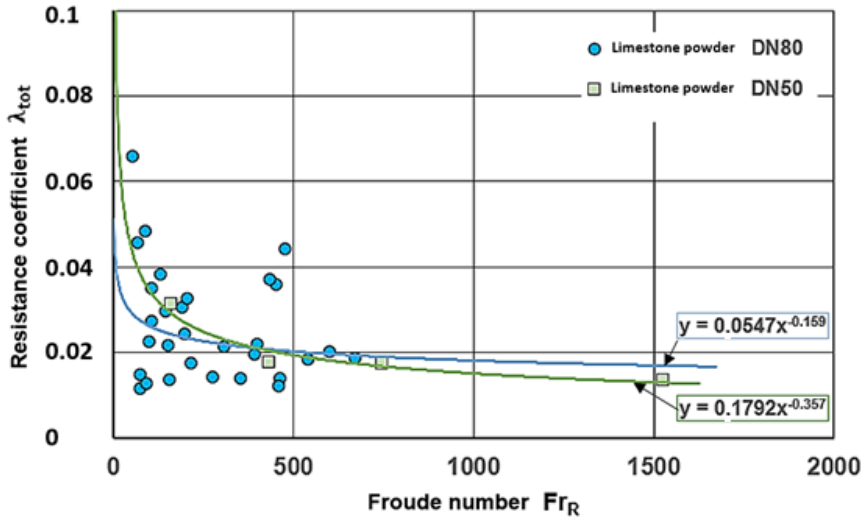

Figure 3. Influence of the special pipeline routing on $\lambda_{tot}(\overline{Fr}_R)$, limestone powder tests.

Figure 4 shows the dependencies of the resistance coefficients $\bar{\lambda}_{S,h}(\overline{Fr}_R)$ of the limestone powder calculated with Eq. (16a) from the measured λ_{tot}-values. The $\bar{\lambda}_{S,h}$-values of the different pipe lengths with the pipe diameter $D_R = 82.5\,mm$ are on a common curve. As with wood powder, the resistance coefficient $\bar{\lambda}_{S,h}$ is also reduced here at given $\overline{Fr}_R$ with increasing pipe diameter D_R. The size of the $\bar{\lambda}_{S,h}$-changes with the pipe diameter D_R is also dependent on the current $\overline{Fr}_R$-number.

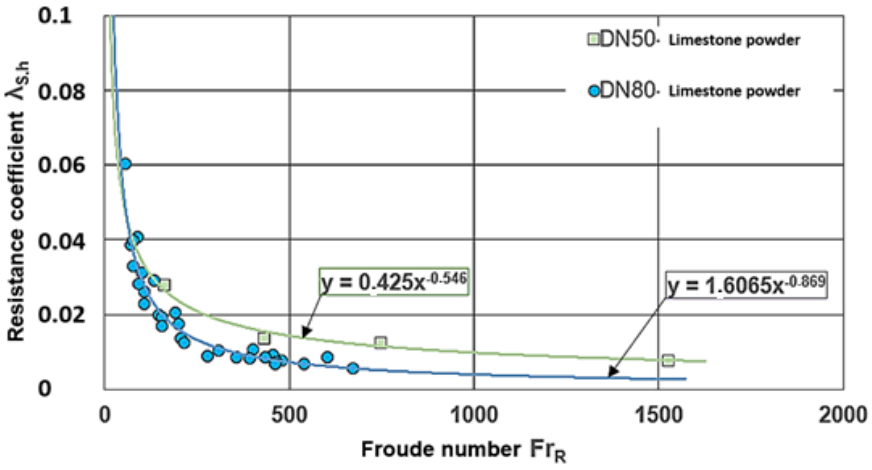

Figure 4. Dependence $\bar{\lambda}_{S,h}(\overline{Fr}_R)$ of limestone powder tests, $D_R = 54.5\ mm$ and $D_R = 82.5\ mm$.

4.4 Scale-Up to Other Conveyor Lines

The following procedure is proposed for the transfer of the pressure loss measurements determined at a test plant, index "V", to a planned operating plant, index "B", with a specified solids mass flow $\dot{M}_{S,B}$ and back pressure $p_{R,out,B}$ at the end of the pipe:

1. Calculation of the average conveying gas velocities $\bar{v}_{F,V}$ of the individual tests using Eq. (19).
2. Calculation of the $\lambda_{tot,V}$-values of the individual experiments with Eq. (1),
3. Determination of the $\bar{\lambda}_F$-values of the individual tests using Eq. (17),
4. Calculation of the $\bar{\lambda}_{S,h}$-values of the individual tests from Eq. (16a),
5. Representation of the test $\bar{\lambda}_{S,h}$-values as a function $\bar{\lambda}_{S,h}(\overline{Fr}_R, \mu, D_R)$ with

$$\overline{Fr}_R = \frac{\bar{v}_{F,V}^2}{g \cdot D_{R,V}} = \frac{v_{F,in,V} \cdot v_{F,out,V}}{g \cdot D_{R,V}} \quad und \quad \mu = \frac{\dot{M}_{S,V}}{\dot{M}_{F,V}} \qquad (20a,b)$$

$\bar{\lambda}_{S,h}(\overline{Fr}_R, \mu, D_R)$ can be represented in a diagram $\bar{\lambda}_{S,h}$ over $\overline{Fr}_R$ with $\mu\ rather\ D_R$ as parameters or can be correlated by a suitable function. The function $\bar{\lambda}_{S,h}(\overline{Fr}_R, \mu, D_R)$ is the basis for the scale-up to a planned operating facility. For the functional dependencies of $\bar{\lambda}_{S,h}$, and $\bar{\lambda}_F$, $f(\bar{\lambda}_{S,h}) = f(\bar{\lambda}_{S,h,V}) = f(\bar{\lambda}_{S,h,B})$ and $f(\bar{\lambda}_F) = f(\bar{\lambda}_{F,V}) = f(\bar{\lambda}_{F,B})$ applies. This means that they can be applied to both the test and the operating plant.

The following steps are then required for the pressure loss calculation of the respective operating system:

1. Specification/Estimation of a Conveyor Pipe Diameter, $D_{R,B}$.
2. Determination of a suitable initial conveying gas velocity $v_{F,in,B}$ (or final velocity $v_{F,out,B}$).
3. Estimation of the pressure loss $\Delta p_{R,B}$ to be expected in the plant.
4. Calculation of the corresponding final velocity $v_{F,out,B}$ of the conveying gas (or initial velocity $v_{F,in,B}$), as well as the resulting mean velocity of gas $\bar{v}_{F,B}$, using $\Delta p_{R,B}$.
5. Determination of the required gas mass flow $\dot{M}_{F,B}$ and the loading μ at the specified solid mass flow rate $\dot{M}_{S,B}$.

6. Calculation of the $\overline{Fr_R}$-number analogous to Eq. (20a) or (19) and determination of the $\bar{\lambda}_{S,h}$-value of the plant from the $\bar{\lambda}_{S,h}(\overline{Fr}_R, \mu, D_R)$-diagram or the correlation equation determined at the test plan.
7. Determination of the $\bar{\lambda}_F$-value of the plant by means of Eq. (17).
8. Recalculation of the $\lambda_{tot,B}$-value of the plant by means of Eq.(16) and $\bar{\lambda}_{S,h}$ from step 11, $\bar{\lambda}_F$ $from$step 12 and the operating data of the planned conveyor system.
9. Calculation of a corrected pressure loss $\Delta p_{R,B,kor}$ with Eq. (1) and $\lambda_{tot,B}$ from step 13.
10. Comparison of the estimated value $\Delta p_{R,B}$ with $\Delta p_{R,B,kor}$: Is $\left|\Delta p_{R,B} - \Delta p_{R,B,kor}\right| > \delta$, where δ is a suitably chosen precision bound, $\Delta p_{R,B} = \Delta p_{R,B,kor}$ is set and jumped back to step 9. This iterative loop is repeated until $\left|\Delta p_{R,B} - \Delta p_{R,B,kor}\right| \leq \delta$ is. Practical calculations show that the iteration after approx. 3 runs turns to a stable final value for $\Delta p_{R,B}$.

The pressure loss calculation of a pneumatic conveying line using the λ_S-method generally requires an iterative approach.

The dependence $\bar{\lambda}_{S,h} \propto 1/D_R^m$ determined by the wood and limestone powder measurements is also observed for other bulk materials [1]. If such solids $D_{R,B} > D_{R,V}$ are used, then the pressure loss of the plant is on the "safe" side means it is greater than necessary, and vice versa.

4.5 Example of Application

4.5.1 Design Data

An intermediate transport system is to be designed for a sandy alumina conveyed in the CP technical centre; minimum conveying speeds are required to calculate a low-wear conveying system.

- Pressure at end of pipe: $p_{out,B} = 1.00\ bar$,
- Design temperature: $T_B = 20℃$,
- Bulk material: sandy alumina, specification according to Table 5.

Table 5. Sandy alumina specification.

Parameter	Unit	Sandy alumina
Mean particle diameter $d_{S,50}$	$[\mu m]$	73
Slope of RRSB graph	$[\alpha_{RRSB}]$	64.8
Loose bulk density ϱ_{SS}	$[kg/m^3]$	1020
Vibrated density ϱ_{SR}	$[kg/m^3]$	1250
Solids density ϱ_S	$[kg/m^3]$	3490
Deaeration time $\Delta t(2\ kg)$	$[s]$	ca. 16
Geldart Class	[-]	B
Particle shape	[-]	Cube, plate, ball (mostly)
Notes	[-]	Turbulent material movement with bubbles.

- Conveying gas: Air, density $\varrho_{Luft}(20℃, 1{,}0\ bar) = \varrho_{F,out,B} = 1.20\,kg/m^3$, dynamic viscosity $\eta_{air}(20℃, 1{,}0\ bar) = \eta_{F,T_B} = 18.24 \cdot 10^{-6}\ Pa \cdot s$,
- Massflow: $\dot{M}_{S,B} = 9\,t/h$,

- Conveying distance: $L_{R,B} = 90\ m$,
- including a vertical height of: $\Delta L_{R,v,B} = 38\ m$,
- Number of deflections recalculated to 90°-bends, see Eq. (14): $N_U = 8$,
- given conveying pipe diameter: $D_{R,B} = 143.0\ mm$ (→ Pipe ∅ $159.0\ mm\ x\ 8\ mm$).

4.5.2 Calculation of the Plant

The further procedure is as described in section 3.3, whereby the $\bar{\lambda}_{S,h}$- test data are already available (→ scale up step 1-5) and Figure 5 below, $D_R = 82.5\ mm$.

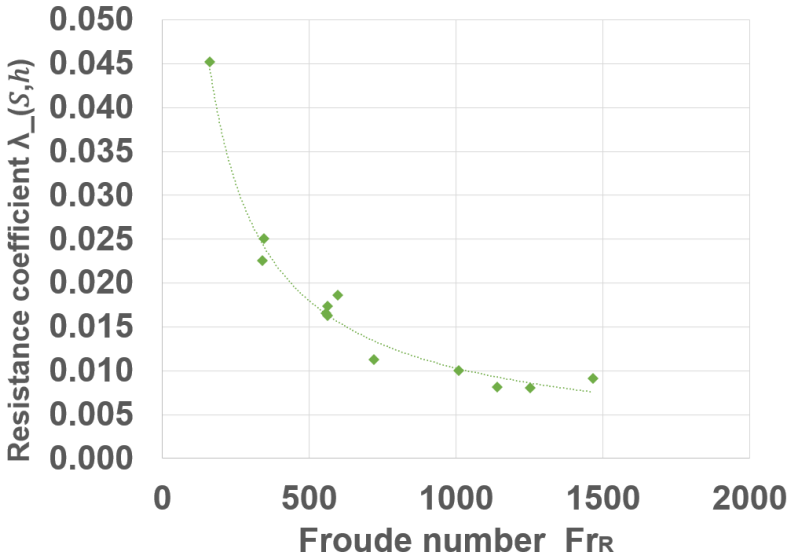

Figure 5. Dependence $\bar{\lambda}_{S,h}(\overline{Fr}_R)$ of sandy alumina tests, $D_R = 82.5\ mm$.

- Lower conveying limit: As a lower limit for stable conveying operation (→ the latter can be checked using the pressure measurement strips from the corresponding conveying tests) as explained in section 3.2, analogue the procedure with Figure 2, the Froude-number of Figure 5 should be $\overline{Fr}_{R,min} \gtrsim 250$ plus a safety distance is used.

Selected:

$$\overline{Fr}_{R,B} = \frac{\bar{v}_F^2}{g \cdot D_R} = 400$$

with

$$v_{F,out} = v_{F,in} \cdot \frac{p_{in}}{p_{out}}$$

$$\overline{Fr}_{R,B} = \frac{v_{F,in} \cdot v_{F,out}}{g \cdot D_R} = \frac{v_{F,in}^2}{g \cdot D_R} \cdot \frac{p_{in}}{p_{out}}$$

generally, follows from this for the initial conveying gas velocity $v_{F,in}$

$$v_{F,in} = \sqrt{g \cdot D_R \cdot \overline{Fr}_{R,B} \cdot \frac{p_{out}}{p_{in}}} \tag{21}$$

where:

$\overline{Fr_R}$	Froude number
$\bar{v}_F$	Mean "empty pipe velocity" of fluid, m/s
p_{in}	Pressure at beginning of conveying line. bar,
p_{out}	Pressure at end of conveying line. bar,
D_R	Diameter of piping, m

The following therefore applies to this plant:

$$v_{F,in,B} = \sqrt{g \cdot D_{R,B} \cdot \overline{Fr}_{R,B} \cdot \frac{p_{out,B}}{p_{in,B}}} = \sqrt{9.81\frac{m}{s^2} \cdot 0.143\ m \cdot 400 \cdot \frac{p_{out,B}}{p_{in,B}}}$$

$$= 23.69\frac{m}{s} \cdot \sqrt{\frac{p_{out,B}}{p_{in,B}}} \qquad (21a)$$

where:

$\overline{Fr_R}$	Froude number
$v_{F,in}$	Gas velocity at inlet, m/s
p_{in}	Pressure at beginning of conveying line. bar,
p_{out}	Pressure at end of conveying line. bar,
D_R	Diameter of piping, m
g	Gravity acceleration, 9.81 *m/s²*

4.5.3 Calculation of Pressure Loss

As fixed values in Eq. (16) to calculation the total resistance coefficient $\lambda_{tot,B}$ of the plant:
$C = 0.70,\ k_v = 1.00,\ (K_U \cdot C) = 0.35$. This results in:

$$\left(\frac{L_{R,h,B}}{L_{R,B}} + k_v \cdot \frac{L_{R,v,B}}{L_{R,B}}\right) = 1.0$$

$$\frac{2}{C} \cdot \frac{L_{R,v,B}}{L_{R,B}} = \frac{2}{0.70} \cdot \frac{38\ m}{90\ m} = 1.2063,$$

$$2 \cdot \frac{D_{R,B}}{L_{R,B}} = 2 \cdot \frac{0.143\ m}{90\ m} = 3.1778 \cdot 10^{-3},$$

$$N_U \cdot K_U \cdot C = 8 \cdot 0.35 = 2.80.$$

The design steps 7 ff of section 3.3 are processed below.
Assumend pressure loss: $\left|\Delta p_{R,B}\right| = 0.40\ bar$, with $p_{out,B} = 1.00\ bar$, $p_{in,B} = 1.40\ bar$ follows.

Initial conveying gas velocity, Eq. (21a):

$$v_{F,in,B} = 23.69\frac{m}{s} \cdot \sqrt{\frac{p_{out,B}}{p_{in,B}}} = 23.69\frac{m}{s} \cdot \sqrt{\frac{1.00\ bar}{1.40\ bar}} = 20.01\frac{m}{s}$$

Conveying gas velocity at the end:

$$v_{F,out,B} = v_{F,in,B} \cdot \frac{p_{in}}{p_{out}} = 22.37\frac{m}{s} \cdot \frac{1.40\ bar}{1.00\ bar} = 28.02\frac{m}{s}$$

Geometric mean value of gas velocities, Eq. (19):

$$\bar{v}_{F,B} = \sqrt{v_{F,in,B} \cdot v_{F,out,B}} = \sqrt{20.01\frac{m}{s} \cdot 28.02\frac{m}{s}} = 23.68\frac{m}{s}$$

Conveying gas mass flow:

$$\dot{M}_{F,B} = \frac{\pi}{4} \cdot D_{R,B}^2 \cdot v_{F,out,B} \cdot \varrho_{F,out,B} = \frac{\pi}{4} \cdot (0.143\ m)^2 \cdot 28.02\frac{m}{s} \cdot 1.20\frac{kg}{m^3} \cdot 3600\frac{s}{h}$$
$$= 1944.08\frac{kg}{h}$$

Specific load:

$$\mu_B = \frac{\dot{M}_{S,B}}{\dot{M}_{F,B}} = \frac{9.0\frac{t}{h} \cdot 1000\frac{kg}{t}}{1944.08\frac{kg}{h}} = 4.63\frac{kg_S}{kg_F}$$

Define the resistance coefficient $\bar{\lambda}_{S,h}$ of the sandy alumina for the operating conditions $\overline{Fr}_{R,B} = 400$, $\mu_B = 4.6$ und $D_R = 82.5\ mm$ with Fig. 5:

$$\bar{\lambda}_{S,h} \cong 0.0215$$

Calculation the resistance coefficient $\bar{\lambda}_F$ of the conveying gas, Eq. (17):

$$\bar{\lambda}_F = 0.3164 \cdot \left(\frac{4}{\pi} \cdot \frac{\dot{M}_{F,B}}{D_{R,B} \cdot \eta_F}\right)^{-1/4}$$
$$= 0.3164 \cdot \left(\frac{4}{\pi} \cdot \frac{1944.08\frac{kg}{h}}{3600\frac{s}{h} \cdot 0.143\ m \cdot 18{,}24 \cdot 10^{-6}\ Pa \cdot s}\right)^{-1/4} = 0.01396$$

Recalculation of the total resistance coefficient $\bar{\lambda}_{tot,B}$ with Eq. (16):

$$\lambda_{tot,B} = \bar{\lambda}_{S,h} \cdot \left(\frac{L_{R,h,B}}{L_{R,B}} + k_v \cdot \frac{L_{R,v,B}}{L_{R,B}}\right) + \frac{\bar{\lambda}_F}{\mu_B} + 2 \cdot \frac{D_{R,B}}{L_{R,B}}$$
$$\cdot \left(C \cdot \frac{v_{F,out,B}}{\bar{v}_{F,B}} + \frac{1}{\mu_B} \cdot \frac{v_{F,out,B} - v_{F,in,B}}{\bar{v}_{F,B}} + N_U \cdot K_U \cdot C\right) + \frac{2}{C} \cdot \frac{L_{R,v,B}}{L_{R,B}} \cdot \frac{g \cdot D_{R,B}}{\bar{v}_{F,B}^2}$$
$$= 0.0215 \cdot (1) + \frac{0.0140}{4.63} + 3{,}178 \cdot 10^{-3}$$
$$\cdot \left(0.70 \cdot \frac{28.02\frac{m}{s}}{23.68\frac{m}{s}} + \frac{1}{4.63} \cdot \frac{28.02\frac{m}{s} - 20.01\frac{m}{s}}{23.68\frac{m}{s}} + 2.80\right) + \frac{1.2063}{500}$$
$$= 0.0393$$

With Eq. (1) a corrected pressure loss $\left|\Delta p_{R,B}\right|_{kor}$ of the plant is calculated. Eq. (1) can be transformed by $(\bar{\varrho}_F \cdot \bar{v}_F) = \dot{M}_F / A_R$ and $\mu = \dot{M}_S / \dot{M}_F$ to:

$$\left|\Delta p_{R,B}\right|_{kor} = \frac{2}{\pi} \cdot \lambda_{tot,B} \cdot \dot{M}_{S,B} \cdot \frac{L_{R,B}}{D_{R,B}^3} \cdot \bar{v}_{F,B} \qquad (1a)$$

$$\left|\Delta p_{R,B}\right|_{kor} = \frac{2}{\pi} \cdot 0.0393 \cdot \frac{9\frac{t}{h} \cdot 1000\frac{kg}{t}}{3600\ s} \cdot \frac{90\ m}{(0.143\ m)^3} \cdot 23.68\frac{m}{s} = 45585.72\ Pa$$
$$= 0{,}456\ bar$$

Repeated insertion of the $|\Delta p_{R,B}|_{kor}$ value determined in each case as the new estimated/start value $|\Delta p_{R,B}|$ into the calculation process shown above leads to the results of the iteration summarized in Table 6. The following applies to all runs: $\overline{Fr}_{R,B} = 400 = const.$. After three iteration steps, the relative error is $(|\Delta p_R|_{kor} - |\Delta p_R|)/|\Delta p_R| < 0.002\%$. The iteration is cancelled, as no exact values can be read from the available $\bar{\lambda}_{S,h}$-diagram, see Figure 5. All data relevant to the system design is printed in bold.

Table 6. Iteration, Pipe $D_R = 143.0\ mm$, unstopped.

Step		$[Nr.]$	1	2	3
$\|\Delta p_{R,B}\|$		$[bar]$	0.400	0.456	0.458
$v_{F,in,B}$		$[m/s]$	20.01	19.64	**19.61**
$v_{F,out,B}$		$[m/s]$	28.02	28.59	**28.59**
$\dot{M}_{F,B}$		$[kg/h]$	1944.08	1983.63	**1983.83**
μ_B		$[kg_S/kg_F]$	4.63	4.54	**4.54**
$\bar{\lambda}_{S,h}$		[1]	0.0215	0.0215	**0.0215**
$\bar{\lambda}_F$		[1]	0.0140	0.0139	**0.0139**
$\lambda_{tot,B}$		[1]	0.0393	0.0394	**0.0394**
$\|\Delta p_{R,B}\|_{kor}$		$[bar]$	0.456	0.458	**0.458**

The calculation described can be accelerated using suitable iteration methods, e.g. selection of $|\Delta p_{R,B}|_{neu} = \left(|\Delta p_{R,B}|_{alt} + |\Delta p_{R,B}|_{kor}\right)/2$. Further information on the design of pneumatic conveyor systems includes [1, 4].

5. Conclusions

A method for transferring the conveying pressure losses determined on a pneumatic test system to an operating system that differs in geometry and routing is presented. For this purpose, the $\overline{Fr}_R = \bar{v}_F^2/(g \cdot D_R)$ variation of the total test resistance coefficient, which is related to an average Froude number and depends on the pipe routing, is converted into a resistance coefficient of the solid that is (as far as possible) independent of the pipeline route and thus can be used for scale-up. From this, in turn, the respective total drag coefficient of the current plant can be determined, taking into account the course/characteristics of the operating system. This allows for an easy scale up. If a system is well known in dimensions and operating data, it is possible to derive from this data the necessary resistance coefficients and design a conveying system.

6. References

1. Peter Hilgraf, *Pneumatic Conveying - Basics, Design and Operation of Plants*, Springer Vieweg, Berlin (2019).
2. Peter Hilgraf, M. Moka, Direct Scaling -Up of pneumatic conveying tests to industrial systems, *Zement-Kalk-Gips*, 2/2023.

3. K. Hirschfeld, Creation of an evaluation model for the detailed scale-up for the design of a real plant and the investigation of a bulk material for the solids velocities in pneumatic conveying, *Bachelor's thesis*, *Hamburg University of Applied Sciences (HAW),* 2022
4. Peter Hilgraf, *Project planning and design of bulk material systems - presentation based on practical examples*, Springer Vieweg, Berlin (2022).